Available online at www.sciencedirect.com

ScienceDirect

JOURNAL OF IRON AND STEEL RESEARCH, INTERNATIONAL. 2016, 23(4): 372-379

A Flow Stress Model for High Strength Steels with Low Carbon Bainite Structure

Bao-sheng XIE[1], Qing-wu CAI[1], Wei YU[2], Shi-xin XU[2], Ban WANG[2]

(1. Collaborative Innovation Center of Steel Technology, University of Science and Technology Beijing, Beijing 100083, China; 2. National Engineering Research Center of Advanced Rolling, University of Science and Technology Beijing, Beijing 100083, China)

Abstract: Two kinds of steels (YP960 and YP690) with low carbon bainite structure were designed, and their flow stress and strain hardening exponents were studied. The results showed that, when Hollomon relation was applied to describe the flow stress, there were significant errors between the experimental and calculated points in specimens tempered below 400 ℃, while a high precision was observed in samples tempered above 400 ℃. Whereas, the modified Voce relation could effectively predict the flow stress as well as the strain hardening exponent at different tempering temperatures, which was verified by unbiased estimators such as maximum relative error (MRXE) and average absolute relative error (AARE). Besides, the modified Voce relation was also applied to estimate the maximum uniform strain, and the correlation coefficients (R) between the experimental data and calculated maximum uniform strain were more than 0.91. The high correlation coefficients indicated that the modified Voce relation could effectively predict the uniform deformation ability of high strength steels with low carbon bainite structure at different tempering temperatures.

Key words: tempering temperature; flow stress; low carbon bainite; Voce type relation; strain hardening exponent

Owing to the severe service environments and the desire of construction machinery for the high strength steels with excellent weldability, YP960 and YP690 steels become the most attractive steels[1-3]. To meet these requirements of construction machinery markets, many steel corporations, such as the Nippon Steel[4], South Korea's POSCO and JFE Steel[1], expected the development of the two kinds of steels. High strength steels that have yield strength above 600 MPa are generally of martensite or tempered martensite structure. To garantee martensite structure, high percentages of carbon and other alloying elements (such as molybdenum and chrome) are the features of conventional high strength steels. Moreover, the common approach to increase the strength of traditional high strength steels is increasing the content of carbon or other alloying elements to improve the hardenability. Nonetheless, high content of carbon and alloying elements leads to a high carbon equivalent (C_{eq}) and deterioration of low temperature toughness and weldability. As contrast to martensitic steels, low carbon bainitic steels are composed of few alloying elements but have excellent hardenability, weldability property and strength, which leads these kinds of steels to be more prevalent[5,6].

Tempering process is related to complex evolutions of microstructure and plays a crucial role in the deformation behavior of high strength steels. Many researchers[3,7,8] conducted intensive studies on the heat treatment (direct quenching (DQ), reheat quenching (RQ) as well as heat treatment online process (HOP)[1,9] for instance), but further studies on the mechanical properties and deformation behavior were neglected. Recently, in view of mobile dislocation, lath boundaries and dissolved carbon and nitrogen atoms, Yan et al.[10] explained the appearance of upper yield point and strain hardening exponent; however, flow stress models for tempe-

Foundation Item: Item Sponsored by National Natural Science Foundation of China (51274036)

Biography: Bao-sheng XIE, Doctor Candidate; **E-mail**: xiebaoshenghql@gmail.com; **Received Date**: December 8, 2014

Corresponding Author: Qing-wu CAI, Doctor, Professor; **E-mail**: caiqw@nercar.ustb.edu.cn

ring process and strain hardening were not involved in the researches, either.

The common flow stress-strain relations include Hollomon type, Swift type and Voce type, etc. Through fitting of the strain and tensile stress during uniform plastic deformation, the parameters in the flow stress-strain relations could be calculated. As the data of Yan et al.[10] shown, the Hollomon equation can be applied to predict the flow stress of the low carbon bainitic YP960 steels. However, there were significant errors between the Hollomon equation and the experimental data, especially in as-quenched and low temperature tempered steels as the data in Ref. [11] indicated. In published references, there are no applicable models for there kinds of steels. Thus, in this paper, two kinds of low carbon bainitic steels with yield strength of about 690 and 960 MPa were designed and manufactured by DQ/ultra fast cooling (UFC) and tempering, then the deformation behaviors of the two steels during uniaxial tension were studied. Besides, based on dislocation density, a model for flow stress and strain hardening exponent was established for the two steels.

1 Experimental

The detailed chemical compositions of the investigated steels are represented in Table 1. The as-received materials were smelted in a 25 kg vacuum induction furnace, and were forged into stocks with sizes of 60 mm × 60 mm × 100 mm. The blocks of YP960 steels and YP690 steels were soaked at 1250 ℃ for 2 h, and hot-rolled to 12 and 16 mm plates in thickness, respectively. The start rolling temperature of finish rolling was below 900 ℃. The YP960 steel plates were directly quenched after rolling, while the YP690 plates were fast cooled to room temperature (cooling rate is about 70 ℃/s). The samples for the tensile test were cut from the plates along the longitudinal direction and then incubated at given tempering temperature for 35 min followed by cooling in air. The tempering temperatures were chosen as 250, 350, 400, 450, 500, 550, 600, and 650 ℃, respectively. Thermal cycles were represented in Fig. 1 for the two materials.

Table 1 Chemical compositions of investigated steels mass%

Steel	C	Si	Mn	Cu	B	Ti	Nb	V	Cr	Mo	Ni	C_{eq}
YP960	0.07	0.164	1.475	0.241	0.0013	0.03	0.055	0.04	0.569	0.147	0.265	0.504
YP690	0.07	0.18	1.79	—	0.0016	0.01	0.06	0.057	0.96	—	0.21	0.586

Note: $C_{eq}=C+Mn/6+(Cu+Ni)/15+(Cr+Mo+V)/5$.

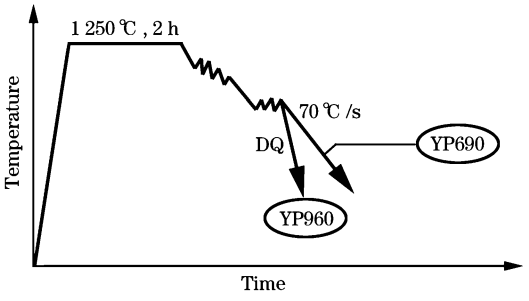

Fig. 1 Schematic drawing of rolling and cooling processes for the two experimental steels

The cylindrical tensile specimens with 5 mm in diameter and 25 mm in gauge length were employed. The tensile tests were performed at room temperature using a CMT-4105 tensile machine, and the crosshead speed was 2 mm/min. Scanning electron microscopy (SEM, Zeiss ultra 55) was used to observe the microstructure of each specimen. The electron backscattered diffraction (EBSD, Zeiss Ultra Plus field emission scanning electron microscope) with step size of 0.12 μm was used to observe the grain boundaries of each specimen. HKL Channel 5 softwares were employed to analyze the results of EBSD measurements.

2 Results and Discussion

2.1 Microstructures

Microstructures of quenched and tempered YP960 steels are shown in Fig. 2. In quenched specimens, the microstructures are mainly lath bainite (LB) and martensite/austenite islands (M/A islands) along the packet boundaries. The microstructure of specimens tempered at 250 ℃ is nearly same with that of the quenched samples. As for samples that were tempered at 450 ℃, the packet boundaries are still distinct, and M/A islands turn out more dispersive and smaller. In samples that were tempered at 550 ℃, some packet boundaries are observed to be blurried, even disappear. In case of samples that were tempered at 650 ℃, the lath boundaries as well as the substructures disappear, but the prior austenite grain boundary (GB_{PA}) and packet boundary still could be distinguished from the SEM images.

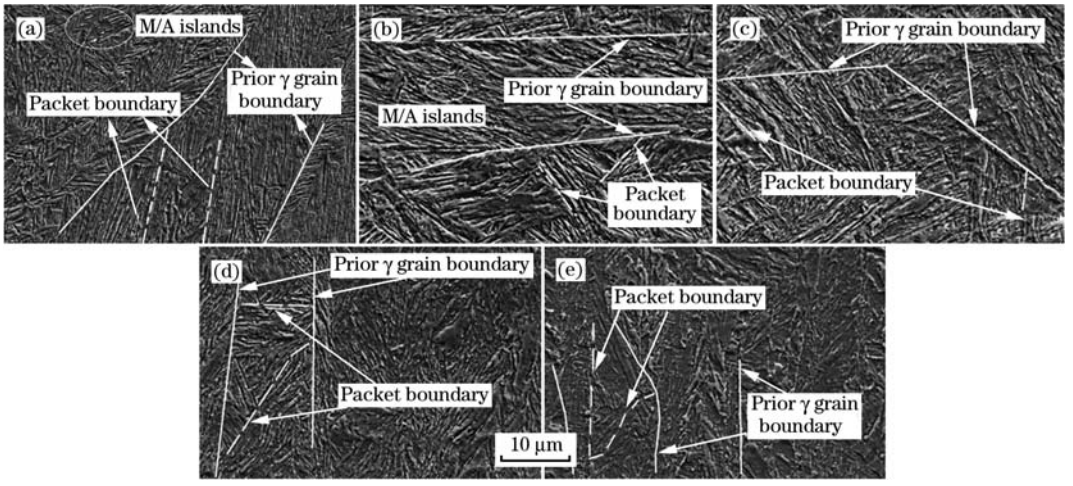

(a) As-quenched; (b) Tempered at 250 ℃; (c) Tempered at 450 ℃; (d) Tempered at 550 ℃; (e) Tempered at 650 ℃.

Fig. 2 Microstructures of YP960 steels tempered at different temperatures

Microstructures of YP690 steels fast cooled and tempered at different temperatures are represented in Fig. 3. The microstructure of the fast cooled YP690 steels is mainly composed of LB and small amounts of ferrite and granular bainite (GB); the bainite packets are intersected each other, and the amount of M/A islands is much more than that of YP960 steels (Fig. 2(a)). It should be noted that, the ferrites in the as-cooled specimens (arrows 1 and 2 in Figs. 3(a) and 3(b)) are distributed along the $GB_{P\Lambda}$ and surround the LB and GB, which are similar to grain boundary allotriomorphic ferrite ($FG_{B\Lambda}$)[12,13]. In specimens tempered at 400 ℃, the packet boundries become obscure, the bainite laths start to bond to each other, and there are only 3—5 packets with remarkably different misorientations in the whole image as a result. In samples tempered at 500 and 600 ℃, the packet boundaries and austenite boundaries disappear; the quasi-polygonal ferrite (QPF, arrows 3 and 4 in Figs. 3(d) and 3(e)) could be observed, and increases in quantity and in size with the increase of tempering temperatures.

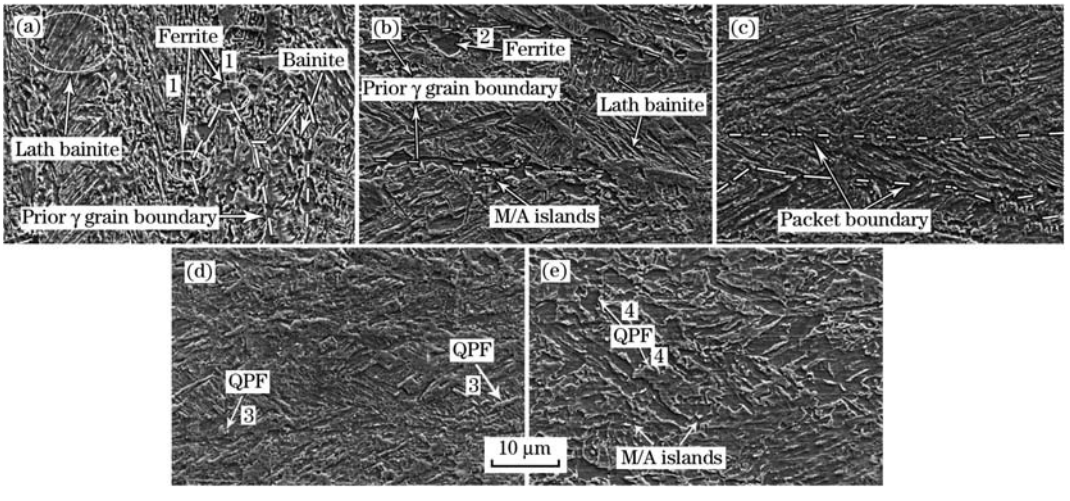

(a) As-cooled; (b) Tempered at 300 ℃; (c) Tempered at 400 ℃; (d) Tempered at 500 ℃; (e) Tempered at 600 ℃.

Fig. 3 Microstructures of YP690 steels tempered at different temperatures

2.2 Flow stress-strain relation

Aiming to describe the strain hardening behavior in the entire range of plastic deformation, a reasonable flow stress-strain relation should be essential. So when the yield strength, the maximum uniform strain and working hardening ability are referred to, a suitable flow stress-strain relation is required. The common flow stress-strain relations belong to Hollomon equation and Voce relation (expressed by Eqs. (1) and (2), respectively). In Eqs. (1) and (2), e is true strain that can be calculated by Eq. (3); S is true stress that can be calculated by Eq. (4); σ

and ε are engineering stress and engineering strain, respectively; K is the strain hardening coefficient; n is strain hardening exponent; μ is the shear modulus ($\mu=80000$ MPa); b is Burger's vector ($b=2.5\times10^{-10}$ m); α is a constant ($\alpha=0.33$); M is Talor's factor ($M=3$); K_2 is recovery rate; and K_1 is related with the dislocation free path (λ) that depends on some microstructural parameters (grain size, spacing between particles and subgrain size, for instance)[14,15].

$$S=Ke^n \tag{1}$$

$$S=\alpha M\mu b\left\{\frac{K_1}{K_2}[1-\exp(-K_2Me)]\right\}^{0.5} \tag{2}$$

$$e=\ln(1+\varepsilon) \tag{3}$$

$$S=\sigma(1+\varepsilon) \tag{4}$$

However, when the Voce type relation was applied to simulate the flow stress of YP690 and YP960 steels tempered above 400 ℃, there were notable errors between the Voce type relation and the experimental results. In order to describe the flow stress of low bainitic steels, a material constant, p, was introduced into the Voce relation[16], and the modified relation was represented as:

$$S=q[1-\exp(-K_2Me^p)]/K_2 \tag{5}$$

Based on the linear relationship between logS and log$e$ in Hollomon relation, a linear regression results in the values in Table 2. By nonlinear curve fitting of the stress-strain curves, the coefficients (q, K_2, p) in modified Voce relation were obtained and represented in Table 2. The comparisons between the experimental data, Hollomon relation and modified Voce relation are shown in Fig. 4. To estimate the forecasting accuracy of the two relations, average absolute relative error (AARE, represented as Eq. (6)) and maximum relative error (MRXE, represented as Eq. (7)) are applied as unbiased estimators to evaluate the precisions of the models. As shown in Table 2, the predicted results by the modified Voce relation approximate well to the real ones, and are more accurate compared to those of Hollomon relation. In samples cooled and tempered at low temperature, the AARE and MRXE of Hollomon relation are more than 1% and 5%, respectively, which implies that Hollomon relation would result in non-

Table 2 Fitting parameters in modified Voce relation and Hollomon relation of YP960 and YP690 steels

Steel	Tempering temperature/℃	q	K_2	p	$AARE_V$/%	$MRXE_V$/%	K	n	n/e_U	$AARE_H$/%	$MRXE_H$/%
YP960	Quenched	13993	11.50	0.6442	0.308	1.82	1835.2	0.130	2.98	2.31	10.4
	250	16991	13.87	0.6260	0.200	0.60	1661.6	0.089	2.12	1.36	5.40
	350	21580	18.57	0.6457	0.150	0.38	1515.7	0.072	2.63	0.72	2.87
	450	8257	7.969	0.4140	0.128	0.29	1162.4	0.032	1.50	0.24	1.20
	550	372	0.003	0.0326	0.221	0.45	1106.0	0.032	0.80	0.21	0.41
YP690	Cooled	14855	14.92	0.694	0.161	1.37	1580.2	0.141	2.95	1.46	6.34
	300	5151	4.736	0.466	0.249	1.16	1499.7	0.114	1.90	1.22	5.12
	400	3377	3.250	0.373	0.248	1.30	1328.3	0.093	1.65	0.77	3.86
	500	407	0.054	0.069	0.230	0.79	1129.1	0.0648	0.92	0.23	0.83
	600	371	0.001	0.066	0.686	1.73	1106.6	0.0649	0.72	0.69	1.73

Note: $AARE_V$ and $MRXE_V$ represent the average absolute relative error and maximum relative error of modified Voce relation, respectively; $AARE_H$ and $MRXE_H$ represent the average absolute relative error and maximum relative error of Hollomon relation, respectively; e_U represents the maximum true strain of uniform plastic deformation.

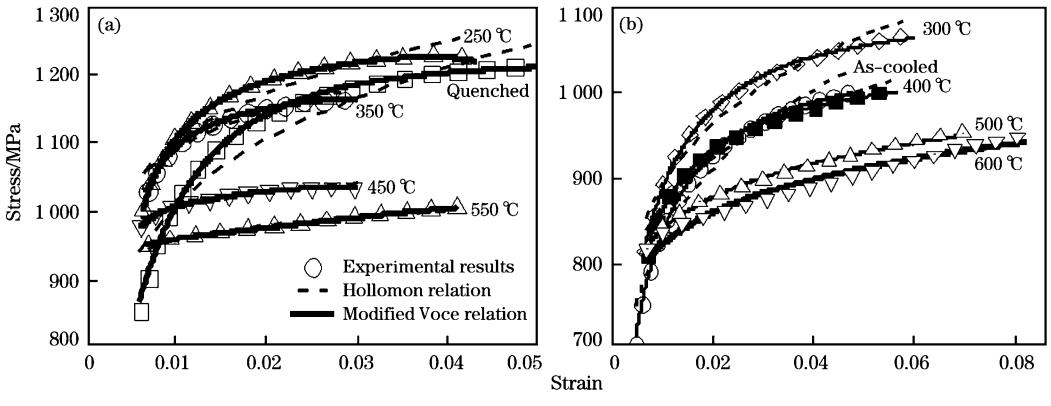

(a) YP960 steel; (b) YP690 steel.

Fig. 4 Comparisons between calculated and experimental flow stress at different tempering temperatures

ignorable errors under these condition. In case of specimens tempered at high temperature, both Hollomon relation and modified Voce relation could predict the flow stress in an exact way, which is in accord with Ref. [10] in aspects of high tempering temperature.

$$\mathrm{AARE}=\frac{1}{N}\sum_{i=1}^{N}\left|\frac{E_i-P_i}{E_i}\right|\times 100\% \quad (6)$$

$$\mathrm{MRXE}=\mathrm{Max}\left|\frac{E_i-P_i}{E_i}\right|\times 100\% \quad (7)$$

where, E_i is the experimental value; P_i is the predicted value obtained by the models above; and N is the total number of data points.

As indicated by Ref. [16], q in Eq. (5) is in inverse proportion to dislocation free path λ ($q=1/(b\lambda)$). Based on geometrically necessary dislocations theory[17], the density of geometrically necessary dislocations (GND) is related with λ and plays decisive roles in the beginning period of plastic deformation. When the samples of YP960 steels were tempered at low temperature, the dislocation is prone to arrange and form the stable dislocation structures; a great amount of fine carbonitrides would start to precipitate as a consequence of high supersaturation of niobium, titanium carbides. Therefore, the density of GND will increase, and λ will decrease, which leads to the increase of q of YP960 steels, as shown in Table 2. However, with the increase of tempering temperature, the precipitates would become coarsening, the lath boundaries and packet boundaries would migrate and disappear, which results in the increase of λ and the decrease of q[16].

Owing to a low content of molybdenum and a relatively low cooling rate, there are few dislocations and more precipitates in the as-cooled YP690 steels than those of the quenched YP960 steels. During low temperature tempering, few dislocations would arrange, and fewer stable dislocation cells would form. Considering stable dislocation cells are low angle grain boundaries (LAGB)[18], the change of dislocation cells at different temperatures can be estimated through the density distributions of grain boundary misorientations (GBM), and the density distributions of GBM could be measured by EBSD tests. From Fig. 5, the density of low angle grain boundaries in YP690 steel is quite less than that of YP960 steel. The LAGB density in YP690 steel decreases with increasing the tempering temperature, even when the tempering temperature is low, which implies few stable dislocation cells formed in YP690 steel. Besides, the relatively long cooling time of YP690 steel leads to low supersaturation degree of niobium, titanium carbides, so fewer precipitates would precipitate when tempering temperature is low. Thus, when the YP690 steel is tempered at low temperature, fewer dislocation cells and precipitates lead to the increase of λ and the decrease of q (see the change of q in Table 2).

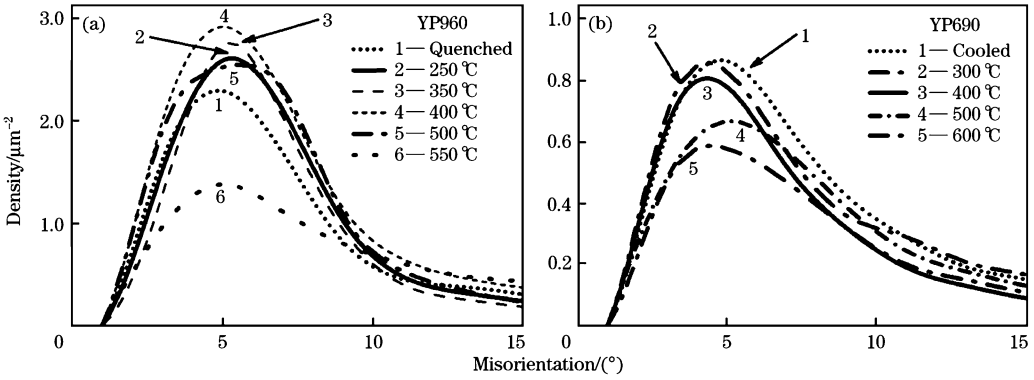

Fig. 5 Density distributions of grain boundary misorientation (GBM) in YP960 (a) and YP690 (b) steels

The coefficient K_2 in Eq. (5) represents the decrease of dislocation density during tensile tests. The decrease of dislocation density comes from the annihilation of dislocation pairs and absorption of dislocations by the sub-boundary[19,20]. As shown in Ref. [21], a large number of dislocation cell structures and substructures would form when low carbon bainitic YP960 steel is tempered at low temperature, which would increase the annihilation of dislocation pairs and absorption of dislocations and make the increase of the coefficient K_2 as a result. When the samples are tempered at high temperature, the opposite sign dislocations on different slip planes tend to climb and annihilate, and the sub-boundaries would decrease due to the mergence of LAGB[22]. Hence, when tempering temperature is above 400 ℃, the dislocation density decreases remarkably. So there are quite few dislocations that would be annihilated

and absorbed during tension, which makes K_2 show significant decline and approach to zero (Table 2). It is worth noting that K_2 of YP690 steel decreases even when tempering temperature is below 400 ℃, and it is because the fewer dislocation cells as well as precipitation in YP690 steel cannot provide sufficient 'traps' of dislocation pairs and are not likely to offset the recovery of the opposite sign dislocations.

2.3 Strain hardening exponent

Strain hardening exponent n was used in Hollomon equation (Eq. (1)) to describe the metal tension deformation, and can be calculated by Eq. (8). In order to develop a deep knowledge of the strain-stress curves, the instantaneous strain hardening exponent (n_ν) was introduced. By the methods of Song et al.[23], the relationship between the instantaneous n_ν and the instantaneous strain (e_ν) is obtained and shown in Fig. 6. The scatter and lines represent the experimental values and calculated values of modified Voce relation, respectively. It could be seen from Fig. 6 that there is no linear relationship between n_ν and e_ν, that is, a single n value is unable to express the deformation behavior under the entire strain[24].

$$n=\frac{\partial \log S}{\partial \log e}=\frac{e\partial S}{S\partial e} \tag{8}$$

Combining Eqs. (5) and (8), the relationship between n_ν and e_ν can be expressed as Eq. (9). Eq. (6)

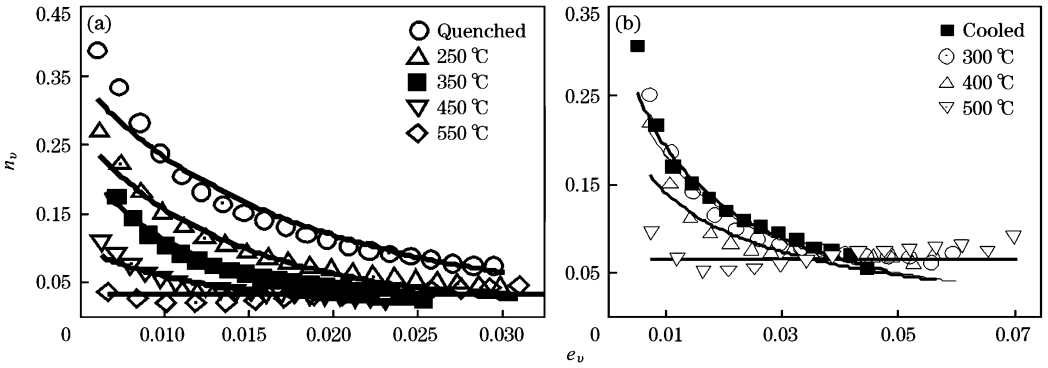

(a) YP960 steel; (b) YP690 steel.

Fig. 6 Comparisons between calculated and experimental $n_\nu-e_\nu$ curves at different tempering temperatures

shows that, the instantaneous n_ν is a function of e_ν, p and K_2, rather than a function of q. The comparisons between the experimental and calculated $n_\nu-e_\nu$ curves are represented in Fig. 6, and the evaluation criteria are shown in Table 3. The root mean square error (RMSE) and mean absolute error (MAE) are determined to be less than 0.019, and the correlation coefficients (R) are above 0.95, indicating that the Voce-type equation can effectively predict strain hardening exponent of the tested steels at different tempering temperatures. If K_2 approaches to zero, the value of n_ν is a constant (Eq. (10)). Therefore, if K_2 is so small that can be neglected, the flow stress is able to be predicted by both of Hollomon relation and modified Voce relation (Eq. (11)), and the coefficient p in modified Voce relation is equal to strain hardening exponent n in Hollomon equation (Eq. (1)). In high temperature tempering (above 500 ℃), K_2 is less than 0.05 and can be neglected, so Hollomon equation can be applied to the prediction of strain hardening exponent. It is noteworthy that the latter part of $n_\nu-e_\nu$ curves in specimens tempered above 450 ℃ shows an uptrend, which is closely related to the strength softening during tempering and the compatible deformation between the 'soft regions' and 'hard regions'[16]. From the above, it is reasonable that there are no significant changes in the $n_\nu-e_\nu$ curves above 500 ℃ and the correlation coefficients (Table 3) are negative.

$$n_\nu=pK_2Me_\nu^p\{[1-\exp(-K_2Me_\nu^p)]^{-1}-1\} \tag{9}$$

$$\lim_{K_2\to 0}n_\nu=\lim_{K_2\to 0}\{pK_2Me_\nu^p[(1-\exp(-K_2Me_\nu^p))^{-1}-1]\}=p \tag{10}$$

$$\lim_{K_2\to 0}S=\lim_{K_2\to 0}\left\{\frac{q[1-\exp(-K_2Me^p)]}{K_2}\right\}=qMe^p \tag{11}$$

On the basis of deformation behavior in uniform plastic stage[25], it is when the true stress and work hardening rate are equal in number (Eq. (12)) that the material starts to deform inhomogeneously. Utilizing Eqs. (8) and (12), one can find strain hardening exponent (n) in Hollomon relation represents the maximum uniform strain (e_U). From Table 2, n and e_U show great differences when tempering temperature is below 400 ℃ but little difference when temperature is above 400 ℃. Besides, the correlation coefficients between n and e_U are less than 0.6 (Fig. 7). So, although strain hardening exponent in Hollomon

Table 3 Error evaluation criteria of calculated n_v-e_v curves at different tempering temperatures

Steel	Tempering temperature/℃	Correlation coefficient	Mean absolute error	Maximum absolute error	Root mean square error
YP960	Quenched	0.978	0.0131	0.0710	0.0193
	250	0.982	0.0097	0.0387	0.0119
	350	0.989	0.0075	0.0170	0.0085
	450	0.960	0.0047	0.0226	0.0062
	550	−0.852	0.0089	0.0160	0.0100
YP690	Cooled	0.978	0.0589	0.0077	0.0127
	300	0.952	0.0471	0.0128	0.0157
	400	0.897	0.0616	0.0129	0.0166
	500	−0.325	0.0411	0.0110	0.0135

equation works well in soft ferritic steels and aluminum alloys, it is considered to be irrelevant to the uniform deformation ability in all the temperature ranges of the tested steels. Substituting Eqs. (5) to (12), one can work out the constraint equation of e_U (expressed as Eq. (13)) determined by modified Voce relation. By means of mathematical software and the data in Tables 2 and 3, e_U at various tempering temperatures can be solved and shown in Fig. 7. Most data points in Fig. 7 are fairly close to the computed lines of modified Voce relation, and the correlation coefficients are above 0.91, which indicates a good relevence between the calculated and experimental e_U. Hence, the modified Voce relation can effectively predict the uniform deformation ability of high strength steels with low carbon bainite structure at different tempering temperatures. In conclusion, if there are adequate data of the uniform deformation, the modified Voce relation may be a valid approach to the prediction for the maximum uniform strain of the high strength steels with low carbon bainite structure.

$$S=\frac{\partial S}{\partial e} \tag{12}$$

$$\exp(MK_2e^p)-MpK_2e^{p-1}=1 \tag{13}$$

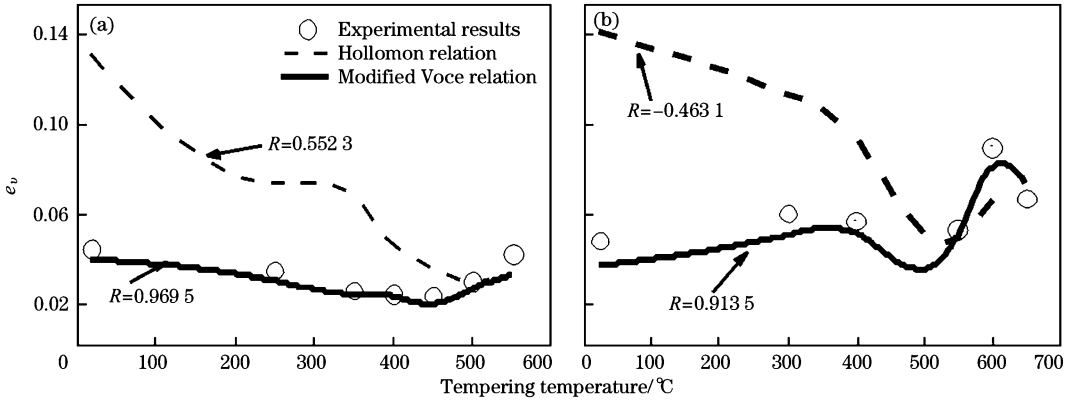

(a) YP960 steel; (b) YP690 steel.

Fig. 7 Comparisons between calculated and experimental maximum uniform strain at different tempering temperatures

3 Conclusions

(1) Two kinds of high strength steels with low carbon bainite structure were designed, and Hollomon relation and a modified Voce relation were applied to describe the flow stress of two experimental steels. The results showed that, applying Hollomon relation to the two tested steels would result in significant errors in low temperature tempered specimens but a high degree of precision in high temperature tempered specimens. The high predictability of the modified Voce relation was also quantified in the aspects of the average absolute relative error and maximum relative error. Considering the effects of tempering on precipitation and dislocation cells, quantitative parameters in modified Voce relation have been expounded.

(2) In order to have a deep knowledge of the strain-stress curves, the instantaneous strain hardening exponent was introduced. There is no linear relationship between the instantaneous strain hardening exponent and the instantaneous strain, so a single strain hardening exponent in Hollomon equation is inadequate to represent the deformation be-

havior under the entire strain. The root mean square error and mean absolute error of the modified Voce relation were determined to be less than 0.0193, indicating that the Voce-type equation can effectively predict strain hardening exponent at different tempering temperatures. When tempering temperature is below 500 ℃, the correlation coefficients are above 0.89. However, when tempering temperature is above 500 ℃, R is negative, which is related to the strength decrease during tempering and the coordinating deformation between the 'soft regions' and the 'hard regions'.

(3) As to the maximum uniform strain, strain hardening exponent in Hollomon relation is proved irrelevant to the uniform deformation ability of the tested steels. With the help of mathematical software, the maximum uniform strain can be evaluated by the modified Voce relation. The correlation coefficients between the experimental and calculated maximum uniform strain are more than 0.91, indicating that the modified Voce relation can effectively predict the uniform deformation ability of high strength steels with low carbon bainite structure at different tempering temperatures.

The authors would like to acknowledge Ms. Dong-xue WANG in Patent Examination Cooperation Hubei Center of the Patent Office, SIPO, and her experimental data of YP690 steels. The authors would also like to thank Mr. Zhen NING, Mr. Lei CHENG and Ms. Qian-li HE for their great help in this paper.

References:

[1] A. Nagao, T. Ito, T. Obinata, JFE Tech. Rep. 11 (2008) 13-18.
[2] Y. Murota, T. Abe, M. Hashimoto, JFE Tech. Rep. 5 (2005) 60-65.
[3] Y. J. Qian, W. Yu, H. B. Wu, Y. H. Yang, J. Univ. Sci. Technol. Beijing 32 (2010) 599-603.
[4] K. Otani, H. Muroka, S. Tsuruta, K. Hattori, H. Kawazoe. Nippon Steel Tech. Rep. 58 (1993) 1-8.
[5] S. C. Wang, R. I. Hsieh, H. Y. Liou, J. R. Yang, Mater. Sci. Eng. A 157 (1992) 29-36.
[6] Z. M. Zhang, Q. W. Cai, W. Yu, X. L. Li, L. D. Wang, J. Iron Steel Res. Int. 19 (2012) No. 12, 73-78.
[7] J. Kang, F. Lu, Z. D. Wang, G. D. Wang, J. Northeast. Univ. 32 (2011) 52-55.
[8] G. C. Hwang, S. Lee, J. Y. Yoo, W. Y. Choo, Mater. Sci. Eng. A 252 (1998) 256-268.
[9] J. Zhang, Q. W. Cai, Y. Q. Fan, H. B. Wu, Trans. Mater. Heat Treat. 32 (2012) No. 4, 55-61.
[10] W. Yan, L. Zhu, W. Sha, Y. Shan, K. Yang, Mater. Sci. Eng. A 517 (2009) 369-374.
[11] F. Lu, J. Kang, C. Wang, Z. D. Wang, G. D. Wang, Iron and Steel 47 (2012) No. 2, 92-95.
[12] L. Li, H. Ding, L. X. Du, H. M. Song, F. Zheng, Acta Metall. Sin. 42 (2006) 1227-1232.
[13] P. G. Xu, H. S. Fang, B. Z. Bai, Z. G. Yang, Acta Metall. Sin. 38 (2002) 255-260.
[14] R. M. Rodriguez, I. Gutiérrez, Mater. Sci. Forum 426-432 (2003) 4525-4530.
[15] A. Ramazani, P. T. Pinard, S. Richter, A. Schwedt, U. Prahl, Comput. Mater. Sci. 80 (2013) 134-141.
[16] B. S. Xie, Q. W. Cai, W. Yu, J. M. Cao, Y. F. Yang, Mater. Sci. Eng. A 618 (2014) 586-595.
[17] M. F. Ashby, Philos. Mag. 21 (1970) 399-424.
[18] Y. N. Yu, Fundamentals of Materials Science, Higher Education Press, Beijing, 2000.
[19] R. Sandström. Acta Metall. 25 (1977) 897-904.
[20] D. W. Suh, J. Y. Cho, K. H. Oh, H. C. Lee, ISIJ Int. 42 (2002) 564-566.
[21] B. S. Xie, Q. W. Cai, W. Yu, J. M. Cao, R. Li, Trans. Mater. Heat Treat. 35 (2014) No. 5, 123-130.
[22] G. X. Hu, X. Cai, Y. H. Rong, Fundamentals of Materials Science, Shanghai Jiaotong University Press, Shanghai, 2000.
[23] Y. Q. Song, Z. P. Guan, P. K. Ma, J. W. Song, Acta Metall. Sin. 42 (2006) 673-680.
[24] L. F. Ramos, D. K. Matalock, G. Krauss, Metal. Trans. 10 A (1979) 259-264.
[25] H. E. Boyer, Atlas of Stress-strain Curves, ASM Int. 1987, pp. 1-10.